NUMERICAL STUDY OF THE PROCESS OF ELECTRODYNAMIC ACCELERATION OF CONDUCTORS

S. A. Kalikhman and A. V. Khorev

UDC 538.24.42

One application of the technology of strong pulsed magnetic fields is in systems for accelerating projectiles to high velocities consisting of capacitive energy storage (CES) and an accelerating system, in which a conductor is accelerated by electromagnetic forces along directing current-conducting rails [1-3]. The need for increasing the maximum determined by the conditions of heating, velocity of bodies with a small transverse cross section and decreasing the intensity of arcing in the moving contact between the conductor and the directing current-conducting rails led to the development of systems with auxiliary transformers [2, 3], in which the current-conducting rails are connected to a secondary winding with a large number of loops, while the current generating the accelerating magnetic field flows along one loop of the primary winding. A variant of such systems is the scheme with a bias magnetization circuit [3], connected in series with the rails and the accelerated conductor, which can be called an autotransformer scheme. Both these schemes preserve the volume density of the accelerating force as the current in the conductor drops owing to an increase in the magnetic-field induction of the bias magnetization circuit. The acceleration process is often studied with the use of the theory of circuits with lumped parameters [4]. In so doing, however, it is impossible to take into account nonlinear diffusion and convection of the field into the conductor and the dynamics of mass reduction on acceleration.

1. Without going into the specific structural details of the autotransformer accelerating systems, in order to understand the factors determining the acceleration process we shall study a one-dimensional model consisting of two-dimensional circuits (Fig. 1). The characteristic inductance of the CES is taken into account by placing the accelerated body at some distance l_{02} from the beginning of the rails. The calculations were performed based on the magnetic induction and the electric field strength, which is equivalent to studying equivalent flat busbars with unit width and unit distance between the rails.

In the coordinate system tied to the outer surface of the solid phase of the conductor, neglecting the displacement currents, the equation describing the interaction of the electromagnetic field has the form [5]

$$\frac{\partial B}{\partial t} = \frac{\partial}{\partial x}\left[\frac{\rho}{\mu_0}\frac{\partial B}{\partial x}\right] - \frac{\partial (uB)}{\partial x}, \tag{1.1}$$

where $\mathbf{B} = -\mathbf{k}B$ is the magnetic field induction vector; $\mathbf{u} = \mathbf{i}u$ is the flow velocity of the liquid phase in the chosen coordinate system; $\mu_0 = 4\pi \cdot 10^{-7}$ H/m; and $\mathbf{i}$, $\mathbf{j}$, and $\mathbf{k}$ are the unit vectors along the x, y, and z axes.

We assume that the resistivity depends linearly on the injected energy right up to the boiling temperature [5]. Then

$$\frac{\partial \rho}{\partial t} = \frac{k\rho}{\gamma\mu_0}\left[\frac{\partial B}{\partial x}\right]^2. \tag{1.2}$$

Here k is a dimensional constant, whose value is presented in [2] for a number of metals and γ is the density of the conductor material.

The equation of motion for the velocity v and the displacement l is

$$\frac{\partial v}{\partial t} = [[B_1 + B_2(-h(t), t)]^2 - B_1^2]/[2\mu_0\gamma h(t)], \quad \frac{\partial l}{\partial t} = v, \tag{1.3}$$

where B_1 and B_2 are the components of the resulting accelerating magnetic field, determined by the bias magnetization circuit and the rails, respectively.

Cheboksary. Translated from Zhurnal Prikladnoi Mekhaniki i Tekhnicheskoi Fiziki, No. 3, pp. 25-29, May-June, 1987. Original article submitted April 29, 1986.

0021-8944/87/2803-0340 $12.50 © 1987 Plenum Publishing Corporation

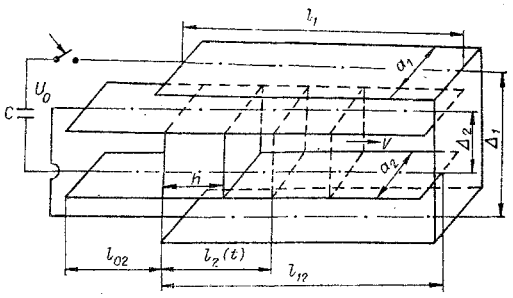

Fig. 1

Since the lateral surface of the accelerated conductor Δh_2 is approximately an order of magnitude smaller than the area of the bias magnetization circuit $l_1\Delta_1$, in what follows we shall neglect the change in the magnetic flux of the bias-magnetization circuit owing to diffusion of the field into the accelerated conductor. Then the left-hand boundary condition at x = −h(t) is determined by the electrotechnical equations for the discharge of the capacitor:

$$U = B_2\frac{a_2}{\mu_0}r + \frac{d}{dt}[w_1B_1l_1\Delta_1 + w_1B_2l_2(t)\Delta_2 + B_2l_{02}\Delta_2] +$$

$$+ \frac{d}{dt}[B_2l_2(t)\Delta_2 + B_1l_2(t)\Delta_2] + E\Delta_2,\quad \frac{dU}{dt} = -\frac{a_2B_2}{\mu_0C} = -\frac{a_1B_1}{w_1\mu_0C},$$

where U is the voltage on the capacitor; C is the capacitance of the capacitor; r is the equivalent total active resistance of the accelerator and the capacitor; w_1, l_1, Δ_1, a_1 are the number of loops, the equivalent lengths, the interbus gap width and the width of the current strip of the bias magnetization circuit; $l_2(t)$, Δ_2, a_2 are the displacement of the accelerated conductor, the equivalent interrail gap width, and the equivalent width of the current-carrying strip of the rails.

For a given construction the equivalent parameters of the one-dimensional computational model are found from the equality of the components of the inductances of the model and of the structure, and the values of the induction are taken in the form $B_1 = k_1\mu_0w_1i/a_1$, $B_2 = k_2\mu_0i/a_2$, where k_1 and k_2 are dimensionless coefficients ($k_{1,2} \in [0, 1]$), determined in each specific case from the results of physical modeling, whose method is described in [6]; i is the discharge current.

Transforming to the electric field strength and the resulting $B = B_1 + B_2$ magnetic induction we obtain the left-hand boundary condition:

$$E(-h(t), t) = E_1(t) - \frac{d}{dt}[B(-h(t), t)(L(t) + l_2(t))] - B(-h(t), t)r\alpha, \tag{1.4}$$

$$L(t) = [w_1w_0^*l_1\Delta_1/\Delta_2 + w_1l_2(t) + l_{02}]/(w_0^* + 1),$$

$$\alpha = a_2/[\mu_0\Delta_2(w_0^* + 1)],\quad w_0^* = w_1a_2/a_1;$$

$$\frac{dE_1}{dt} = -B(0, t)/[\mu_0(w_0^* + 1)C_1],\quad C_1 = C\Delta_2/a_2,\quad E_1 = U/\Delta_2. \tag{1.5}$$

The main boundary condition at x = 0 is B(0, t) = $B_1(t)$. The initial conditions are U = U_0, B(x, 0) = 0, E(x, 0) = 0, $l_2(0) = l_{02}$, v(0) = 0 at t = 0.

The integration is carried out up to the moment t_1, at which $l_2(t_1) = l_{12}$, where l_{12} is the length of the rails along which the acceleration occurs.

The system (1.1)-(1.5) must be supplemented by equations describing the change in the mass of the accelerated conductor during acceleration. As shown in [7, 8], when a strong pulsed magnetic field interacts with the conductors the change in the geometric dimensions of the conductor is associated with the ejection of matter from the skin layer owing to "fast" explosion (loss of conductivity of the metal vapor) and "slow" explosion (ejection of the melted metal along the lines of force).

We take the first mechanism into account by assuming that the conductivity is lost in a jump-like fashion, if the heat content per unit volume exceeds Q_1 – the heat of sublimation (idealized explosion of the skin layer).

We neglect points of the conductor where $Q > Q_1$. Assuming the flow of liquid metal to be stationary and neglecting the nonuniformity of the internal pressure in it, from Bernoulli's law we write the velocity of the

flow of liquid metal in the z direction in the form $v_1 = (2p_1/\gamma)^{1/2}$ (p_1 is the pressure at the boundary of the liquid and solid phases).

From the condition that the liquid is incompressible, taking into account the fact that metal can be ejected only along the z coordinate, for the velocity of the surface of the conductor we obtain

$$u_1 = 2v_1h_1/a_2.$$

Here h_1 is the extent of the liquid phase (the distance from the surface of the conductor to the point where the heat-content per unit volumes equals Q_2 – the total specific heat content of the liquid phase); the factor of two takes into account the ejection of metal on both sides. We give the linear distribution of the velocity in the liquid layer in the form $u(x, t) = u_1(1 - |x|/h_1)$.

The distribution adopted for the velocity does not lead to large errors, since preliminary calculations showed that $u \ll c$, where c is the velocity of sound in the liquid metal, while the extent of the liquid phase $h_1 \ll h$.

Using d'Alambert's principle and the condition of equilibrium, for the internal pressure p(x, t) we find

$$p(x, t) = -\int_{-h}^{x} (f_1 - f_2)\, dx,$$

where f_1 and f_2 are the volume density of the electromagnetic and inertial forces:

$$f_1 = -\frac{B(x, t)}{\mu_0}\frac{\partial B(x, t)}{\partial x}, \quad f_2 = -\frac{B^2(-h, t) - B_1^2(t)}{2\mu_0 h}.$$

In the case when $p_1 > 0$, tensile forces, which above some threshold value detach the layer of liquid metal from the solid surface, arise at the boundary of the liquid and solid phases. Thus for $p_1 > \sigma_e$ (σ_e is the detachment stress, determined by the surface tension and the viscosity; in our calculations, since the loads are impulsive, it is assumed that $\sigma_{eAl} = 10^2$ Pa) a layer of extent h_1 is ejected and the boundary of the surface moves onto the boundary of the solid phase.

The computational model adopted does not take into account all processes occurring in the solid, liquid, and vapor phases: the three-dimensional nonstationary (wave) character of the expansion, the development of MHD instabilities in the liquid metal, shock waves, and brittle fracture of the solid phase. However, it not only reflects correctly the threshold character of the processes and the basic aspects of the phenomenon as a whole, but, unlike [3, 5], it also enables following the dynamics of mass reduction and the change in the phase (percent ratio of the solid, liquid, and vapor phases) state of the conductor during the acceleration process, which makes it possible to study the relationship between the reduction in the mass of the conductor and the electrical parameters of the discharge circuit and the operating efficiency of the accelerator.

2. The system of equations derived for given boundary and initial conditions was solved in a dimensionless form by the method of finite differences employing a purely implicit scheme [9, 10]. In so doing, the method of separate iterations for a completely conservative difference scheme was employed [9].

The nonlinearity of Eq. (1.1) was taken into account by the method of successive approximations, in which the values of the unknown functions were taken from the preceding iterations.

The following were used as the base quantities: $C^* = C_1$, $x^* = (C_1\rho_0^2/\mu_0)^{1/3}$, $t^* = (x^*)^2\mu_0/\rho_0$, $B^* = (2Q_1\mu_0)^{1/2}$, $E^* = B^*\rho_0/(\mu_0 x^*)$, $r^* = \rho_0/x^*$.

The choice of x^* – the equivalent thickness of the skin layer for maximum possible frequency of the discharge – as a base quantity makes it possible to employ a spatial grid step h such that the change in the field strength within this interval would ensure the required computational accuracy. The parameters of the solution are as follows: $e_0 = U_0/(\Delta_2 E^*)$, $\varkappa_0 = h/x^*$, $\varkappa_1 = h(t_1)/x^*$, $\varepsilon_{02} = l_{02}/x^*$, $\varepsilon_1 = l_1/x^*$, $\varepsilon_{12} = l_{12}/x^*$, $\xi = Q_2/Q_1$, $\sigma = \rho_0^2\gamma/(2\mu_0 Q_1)$, $\nu = 2\mu_0 Q_1 k/(\rho_0\gamma x^*)$, $\mu = rx^*/\rho_0$ for variable $\varkappa = h(t)/x^*$, $\varepsilon_2 = l_2(t)/x^*$, $V = vt^*/x^*$.

We shall start the analysis of the computational results with the scheme without a bias-magnetization circuit ($w_1 = 0$). We studied an aluminum conductor with the material characteristics presented in [5]. Figures 2 and 3 show the values of the efficiency of conversion of the energy stored in the capacitor into the kinetic energy of the accelerated body and the velocity and mass of the conductor, scaled to its starting value, as a function of ε_{12}, for different values of $\varkappa_0$ [for curves 1 and 5, $\varkappa_0 = 38$; 2, 6 – 76; 3, 7 – 191; 4, 8 – 477 for $\xi = 9.16 \cdot 10^{-2}$, $\sigma = 2.43 \cdot 10^{-17}$, $\nu = 0.1 \cdot 10^{-2}$, $\mu = 0$, $\varepsilon_{02} = 91$, $e_0 = 1.07 \cdot 10^{-1}$]. Comparison of the results in

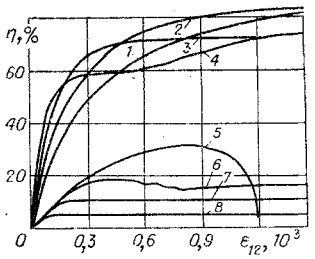

Fig. 2

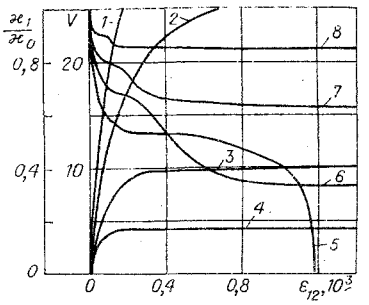

Fig. 3

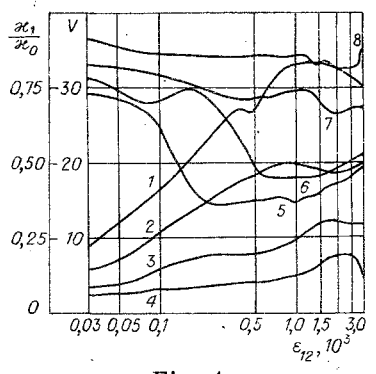

Fig. 4

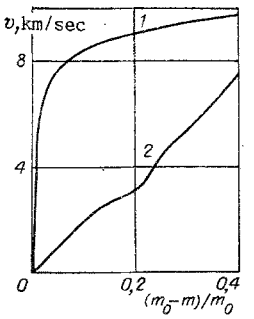

Fig. 5

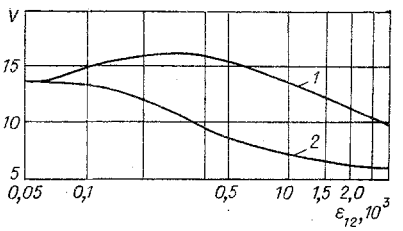

Fig. 6

the case when nonlinear diffusion and the mass reduction are taken into account (curves 5-8 in Fig. 2) and the linear approximation with constant mass (curves 1-4) shows that in the second case the values of the efficiency are too high, and in addition the change in the mass of the conductor during the acceleration process has the greatest effect.

The decrease in the achieved velocity compared with the calculation with constant mass is greatest for high current rise rates and extended conductors ($e_0 > 1.07 \cdot 10^{-1}$, $\varkappa_0 > 100$, $\varepsilon_{02} < 91$). In this case, initially, when the velocity and displacement of the conductor are small, diffusion of the pulsed magnetic field is accompanied by intense erosion. The reduction in the size of the body, which changes the magnetic flux associated with the conductor, gives rise to the appearance of a counter emf, which limits the discharge current and significantly (up to 100%) decreases the velocity achieved. In other words, the change in the inductance of the discharge circuit is determined by the mass lost by the accelerated conductor. For the lowest current rise rates and the smallest lengths (masses) of the conductors, by the time at which the dimensions of the body begin to change the conductor can move along the rails and the contribution of the counter emf decreases.

In all states studied (3 kV/cm $\leq E_1 \leq$ 30 kV/cm; $5.5 \cdot 10^{-2}$ F $\leq C_1 \leq$ 5.5 F; 2.16 g $\leq m_0 \leq$ 10.8 g; $0.48 \cdot 10^{-2}$ m $\leq l_{02} \leq 0.48 \cdot 10^{-1}$ m) the mass of the accelerated body decreased primarily owing to the ejection of the liquid phase – "slow explosion." The pressure in this case did not exceed the dynamic yield stress [11], which makes it possible to ignore in the mathematical model the deformation of the solid phase.

The bias-magnetization circuit reduces the magnetic induction of the rails, while the diffusion of the magnetic field of the bias-magnetization circuit into the conductor from both sides gives rise to additional heating

and mass loss at the front of the projectile. The results of calculations of the values of the velocity (curves 1-4) and the change in mass (curves 5-8) at the end of the rails for $w_1 = 1$, presented in Fig. 4 ($1 - \varkappa_0 = 38$; 2 – 76; 3 – 191; 4 – 477, $e_0 = 1.07 \cdot 10^{-1}$, $\xi = 9.16 \cdot 10^{-2}$, $\sigma = 2.43 \cdot 10^{-17}$, $\nu = 0.1 \cdot 10^{-2}$, $\mu = 0$, $\varepsilon_{02} = 91$), show that there are values of the parameter ε_{12} for which the mass loss is maximum. As an example Fig. 5 shows the results of the calculation of the acceleration of an aluminum body $m_0 = 4.32$ g with the dimensions 15 × 15 × 7 mm on a setup with an energy store of 500 kJ, $U_0 = 30$ kV, and $U_0/L_0 = 10^{13}$ A/sec for $l_1 = l_{12} = 0.1$ m [$(m_0 - m)/m_0 = 0.4$ corresponds to escape of the body) for an accelerator with a bias-magnetization circuit and a railtron (curves 1 and 2). Comparison of the schemes with and without a bias-magnetization circuit, carried out for the regime with a 30% mass loss (Fig. 6, curves 1 and 2, respectively, and the same computational parameters as for Fig. 4), demonstrates the advantages of autotransformer schemes in regimes with intense mass loss during the acceleration process.

LITERATURE CITED

1. F. D. Rosen, "A magnetically augmented rail gun," 7th Symposium on Hypervelocity Impact, Tampa (1964).
2. V. F. Agarkov, V. N. Bondaletov, et al., "Acceleration of conductors up to hypersonic velocities in an impulsive magnetic field," Zh. Prikl. Mekh. Tekh. Fiz., No. 3 (1974).
3. V. N. Bondaletov, S. A. Kalikhman, and V. N. Fomakin, "Computer study of the efficiency of different designs of accelerators for high-velocity conducting projectiles," in: High-Voltage Impulsive Technology [in Russian], Cheboksary (1975), No. 2.
4. G. A. Shneerson, Fields and Transient Processes in Superstrong-Current Apparatus [in Russian], Énergoizdat, Moscow (1981).
5. G. Knopfel', Superstrong Impulsive Magnetic Fields [Russian translation], Mir, Moscow (1972).
6. K. S. Demirtchyan, Modeling of Magnetic Fields [in Russian], Énergiya, Leningrad (1974).
7. G. A. Shneerson, "Theory of electric explosion of a skin layer in a superstrong magnetic field," Zh. Tekh. Fiz., 13, No. 2 (1972).
8. Yu. N. Bocharov, A. I. Kruchinin, and G. A. Shneerson, "Choice of parameters of capacitive storage for the generation of a superstrong magnetic field in exploding solenoids with small volume," Vestn. Khar'kov Politekhn. Inst., No. 123, No. 4 (1977).
9. A. A. Samarskii and Yu. P. Popov, Difference Schemes for Gas Dynamics [in Russian], Nauka, Moscow (1975).
10. N. N. Kalitkin, Numerical Methods [in Russian], Nauka, Moscow (1978).
11. V. G. Belan, S. T. Durman, et al., "Energy losses due to plastic deformation accompanying the compression of a cylindrical shell," Zh. Prikl. Mekh. Tekh. Fiz., No. 2 (1983).